A Study on Indoor Pedestrian Localization Algorithms with Foot-Mounted Sensors

Michailas Romanovas*, Vadim Goridko*, Ahmed Al-Jawad*, Manuel Schwaab*, Lasse Klingbeil†
Martin Traechtler*, Yiannos Manoli*‡
*Hahn-Schickard-Gesellschaft Institute of Microsystems and Information Technology (HSG-IMIT)
Wilhelm-Schickard-Straße 10, 78052 Villingen-Schwenningen, Germany
email: michailas.romanovas@hsg-imit.de
† Institute of Geodesy and Geoinformation, Rheinische Friedrich-Wilhelms-Universitaet Bonn
Nußallee 17, 53115 Bonn, Germany
‡, Fritz Huettinger Chair of Microelectronics, Department of Microsystems Engineering (IMTEK)
Albert-Ludwigs-Universitaet Freiburg, Georges-Köhler-Allee 101, 79110 Freiburg, Germany

***Abstract*—The work presents a foot-mounted sensor system for a combined indoor/outdoor pedestrian localization. The approach is based on a zero-velocity update scheme formulated as an Extended or Unscented Kalman filter with quaternion orientation representation and employs a custom low-cost sensor unit. Both filters are compared in terms of speed and accuracy on a representative trajectory. A detailed discussion is provided with respect to different filter state formulations, stance still detection mechanisms and associated filter parameters. The presented pure inertial system is augmented with magnetic field measurements for heading correction. The challenging localization scenario with an elevator is addressed by augmenting the system with a barometric pressure sensor for height error correction. The work also demonstrates how the basic algorithm version can be extended with reference systems such as GPS and passive RFID tags on the floor for absolute position drift correction.**

***Index Terms*—Indoor Localization, Pedestrian Navigation System, Zero Velocity Update Method, Unscented Kalman Filter, Extended Kalman Filter, Inertial Measurement Unit.**

I. Introduction

The location information is often considered to be a fundamental requirement for ubiquitous and pervasive computing where the indoor pedestrian localization is becoming an important research field of an enormous potential for applications with context aware services. Although a reliable outdoor localization can be addressed with GNSS-based techniques, their usage is mainly limited to open areas with a reliable access to satellite signals. The indoor or mixed indoor/outdoor scenarios seem to be far more challenging as the GNSS signals are usually too weak to penetrate the buildings. A number of approaches are currently competing to become an indoor alternative to GNSS systems in terms of the reliability, ubiquity and, of course, costs.

An increasing attention to the pedestrian localization problem can be also attributed to a recent development in affordable wearable computing platforms. Smartphones and tablet PCs are the examples of such systems, which are powerful enough to perform sensor signal acquisition, preprocessing and run reasonably sophisticated estimation and sensor fusion algorithms in real time. The availability of a GPS receiver, inertial and magnetic sensors, Wi-Fi, Bluetooth as well as access to the maps and other information are making them perfect candidates to serve as the basis for pedestrian localization systems.

Currently none of the available technologies alone can completely satisfy the accuracy, flexibility, scalability and cost requirements for pedestrian indoor localization within an uncontrolled environment and combinations of several complementary technologies are often employed [1]. Complementary sensing modalities are usually combined using the Recursive Bayesian Estimation (RBE) framework [2], which permits to treat sensor imperfections, dynamical model uncertainties and available heuristic information in a consistent way, enabling a performance, which is in general not achievable with any single sensor type.

A reliable indoor pedestrian localization can be extremely helpful for emergency first responders such as fire-fighters, where one can not rely only on localization methods based on the external infrastructure such as Wi-Fi while the availability of the power can not be ensured. Although a basic localization can be performed using only smartphone/tablet PC built-in sensors (i.e. accelerometer, compass, WiFi and GPS), such methods can often provide only a very rough position information. One could try to avoid the external referencing system by adopting integrated pedestrian dead-reckoning (PDR), where the inertial sensors (e.g. accelerometer and gyroscopes constituting the Inertial Measurement Unit - IMU) provide an internal independent reference, immune to interference and signal shadowing. However, an affordable inertial system can be hardly used for any longer time period due to fast accumulating integration errors. Although additional sensors such as a magnetic compass are often integrated into the inertial modules to bound the heading error, an external referencing is still necessary. Note that every additional sensor comes at its own costs such as increased weight and size of the system, power consumption, requirements for infrastructure and associated maintenance costs.

The work presents a foot-mounted system for indoor and mixed indoor/outdoor pedestrian localization, where ultra low-cost commercial inertial and magnetic sensors are fused using

978-1-4673-1954-6/12/$31.00

Unscented and Extended Kalman filters. The designed system is able to provide a reliable position and orientation for a reasonably long time which was before considered feasible only when using more expensive IMUs. The performance of the system is demonstrated for several representative indoor/outdoor scenarios and is evaluated with respect to different models and filter settings. Some of the algorithm's intrinsic accuracy issues are addressed by augmenting the system with magnetic and barometric pressure sensors, a passive RFID tag reader and the GPS for outdoor walking segments. Here RFID was chosen as a low-cost alternative to reference positioning based on Wi-Fi due to its flexibility, low-cost and ability to handle potential power constraints such as blackouts during emergency situations [3].

The remainder of the paper is structured as follows: section II provides a brief discussion on several of the related approaches. Section III presents some mathematical details of the developed scheme along with the fusion filter and dynamical models. A general system concept and the associated hardware/software are explained in Section IV with the results provided in Section V. Section VI concludes the paper and presents an outline for future work.

II. Related Work

A variety of systems have been proposed to address the problem of location determination of persons and objects within indoor environments [4], [5]. While for robotics applications a fairly good performance can be achieved using accelerometers, odometers and angular rate sensors, the approach can not be applied directly for pedestrian localization. One of the most popular solutions is to adopt a simple version of the PDR approach, where the steps are detected by monitoring the accelerometer's output and the person's position is moved by the estimated step length in the direction obtained from the magnetic compass and/or gyroscope. These approaches have to be often tuned for a particular user and can still fail for unusual scenarios such as crowded environments, uphill/downhill walking etc., where the assumptions regarding the walking pattern are violated.

Unfortunately, unaided PDR is sensitive to sensor imperfections and can be used for a very coarse localization only [6], [7]. Methods with combined absolute and relative (inertial) referencing are believed to be more effective in terms of cost and performance with numerous approaches reported using Ultra-Wide-Band (UWB) [8], [9], WLAN [10], RFID etc. For some of the systems above severe constraints for larger scale deployment do exist including high equipment costs, calibration (e.g. fingerprinting for WLAN) and maintenance efforts. By augmenting the absolute reference systems with the inertial sensors and map information one can significantly increase the distance between the positions where the absolute referencing is mandatory [3], [10].

The simplest pedometer-based systems are counting steps and the travelled distance is estimated from the knowledge of an average step length [11]. Although an original pedometer is not able to differentiate between varying types of gait, some kinematic approximations can be adopted for online estimation of an actual step length [12]. The empirical information in step detection and length estimation could easily fail for users with different gait patterns or if the user moves in any other way than his/her normal walking pattern.

The presented work addresses the pedestrian indoor localization using a different strategy, where the IMU and additional sensors are mounted on a foot. The approach employs the assumptions regarding the human foot dynamics and is able to limit the position estimation error to grow only linearly in time. The presented method, commonly referred as the 'Zero Velocity Update' (ZUPT), dramatically decreases the position error by allowing the system to navigate in an open loop for time periods shorter than 1 second (i.e., the typical step duration during normal gait conditions), resetting the estimated velocity when the stance phase of the step is detected [13]. Note that the residual position error is not completely eliminated and remains in general unbounded for an unaided system [7]. The overall fusion concept becomes feasible as the correlation information is introduced by the dynamical model which corrects retrospectively the sensor imperfections.

The original technique of [13] is nowadays widely adopted throughout the research community. Most of the approaches reported so far [3], [4], [11], [14], [15] are actually using only relatively expensive and well calibrated MEMS IMUs with the price often exceeding 1000$ per unit. For those who adopt truly custom and low-cost IMUs (e.g. [7]), the results of a pure unaided inertial navigation are often poor even for a shorter navigation time. The original framework of [13] was extended in numerous recent works of other authors. For example, the work [16] extended the framework with the GPS position measurements, while a validation mechanism for magnetic disturbance detection with cascaded estimation architecture was suggested in [17], [18]. In the series of works of Jimenez [19], [20] the technique was further improved with advanced motion models and restricting the pedestrian to follow mainly straight trajectories. The authors in [15] suggested combining the shoe-mounted IMU with a high resolution, thin and flexible biomechanical ground reaction sensor to improve the robustness of the detection of zero-velocity phases. According to the authors, the true zero velocity occurs as some point around the midstance subphase after all rolling contact of the foot with the ground has been reached, which is often not properly detected by the schemes solely based on inertial sensing, resulting in intrinsic zero-velocity bias negatively affecting the performance of the overall system. A combination of the approach with building information has been reported in [3], while [14] fused the inertial information with the map to constrain the heading and match the orientation of the building. The latter was obtained after processing the original street level image of the environment. The approach of Jimenez was further extended with the information from Structure-From-Motion (SFM) [21], where a decoupled EKF approach was adopted. While one EKF was used within the original INS module, an additional higher-level EKF was developed to fuse the position estimates from INS and SFM. The work

[7] augmented the classical EKF+ZUPT strategy with passive RFID tags. Unfortunately, the RFID position information was not incorporated in a statistically sound manner, but a simple affine transform was used to rotate and scale the trajectory between the current and previous RFID points.

III. Methods

A. Recursive Bayesian Estimation and Kalman Filter

The pedestrian localization can be formulated as a state estimation problem of the system [22]:

$$x_k = f(x_{k-1}, u_k, w_k), \quad (1)$$
$$z_k = h(x_k, \epsilon_k), \quad (2)$$

where $x_k \in \mathbb{R}^n$ is the state at time t_k with the associated measurement $z_k \in \mathbb{R}^m$, $f(\cdot)$ and $h(\cdot)$ are the nonlinear system process and measurement functions respectively, w_k and ϵ_k correspond to the process and measurement noises and u_k stands for control input. Within the framework of RBE [2] the estimation of the state x_k at time t_k is based on all the measurements $Z_k = z_0, \ldots, z_k$ up to that time and is represented as a probability density function (*pdf*) $p(x_k|z_0, \ldots, z_k)$ to be calculated recursively using 2 steps:

Prediction The *a priori* probability $p(\tilde{x}_k) = p(x_k|Z_{k-1})$ is calculated from the last *a posteriori* probability $p(x_{k-1}|Z_{k-1})$ using the process model $p(x_k|x_{k-1})$:

$$p(\tilde{x}_k) = \int p(x_k|x_{k-1})p(x_{k-1}|Z_{k-1})dx_{k-1}. \quad (3)$$

Correction The *a posteriori* probability $p(x_k|Z_k)$ is calculated from the *a priori* probability using the measurement model $p(z_k|x_k)$ and the current measurement z_k:

$$p(x_k|Z_k) = \frac{p(z_k|x_k)p(x_k|Z_{k-1})}{p(z_k|Z_{k-1})} = \eta \cdot p(z_k|x_k)p(\tilde{x}_k). \quad (4)$$

Various implementations of RBE algorithms differ in the way the probabilities are represented and transformed in the process and measurement models [2]. The ZUPT-based localization problem is inherently nonlinear and accordingly one of the nonlinear filters has to be adopted.

Within the EKF, the models are linearized through a first-order Taylor series expansion of the process/measurement models around the current state estimate. Although the original nonlinear functions are used for the state transition and measurement prediction, the covariances are approximated by calculating the Jacobian matrices with respect to the current state estimate (and/or noise if necessary). The general algorithm structure is based on the Kalman filter equations. For well-defined continuous transition models, where the functions can be well approximated as linear during the sampling period, the EKF performs reasonably well and is often considered as de-facto standard for navigation applications. A more detailed discussion on classical EKF can be found in [2]. Note that the original ZUPT algorithm [13] as well as most of the other works [18] is based on the EKF in error-state formulation. Unlike the original work we use a full-state EKF formulation. Fortunately, the final Jacobians are quite sparse and the calculations within a single filter cycle are considerably less demanding compared to the processing required by the Unscented Kalman filter (UKF).

As an alternative to EKF-based filter, we demonstrate the implementation using an UKF, where the probability distribution is approximated by a set of so-called σ-points in the state space, deterministically selected to preserve the Gaussian properties of the distribution under nonlinear transformations. The points are propagated through the original nonlinear process and measurement equations and no Jacobians have to be calculated. Although the filter is believed to have better statistical properties [23], [24], it is more computationally demanding compared to EKF. Some methods exist for optimizing the UKF with respect to computational demand, numerical stability etc., such as its square root versions or adoption of Spherical Simplex σ-points [25].

Below we briefly describe the process model which is a straightforward implementation of the classical INS strapdown integration, and a number of measurement models incorporating various sensors and relevant motion constraints. The basic idea behind the overall framework is to integrate the inertial sensors with the rate of their availability (>100Hz) using the INS mechanization model and perform the measurement update whenever an additional information in the form of GPS/RFID location or stance still detection is available.

B. The Models

A sketch of the process model can be seen in Fig. 1, where the prediction step is based on a simplified INS mechanization with the state of the system given as:

$$x_k = [q_k, v_k, p_k, b_{\omega,k}, b_{a,k}]^T, \quad (5)$$

where q_k is the orientation quaternion, v_k and p_k are the velocity and the position in the navigation frame and $b_{\omega,k}$ and $b_{a,k}$ are the gyroscope and accelerometer offsets. The process model of the quaternion is a discrete integration of the input angular rate:

$$q_k = \frac{1}{2}\int_0^{\Delta t} \Omega(\omega)\, q_{k-1} dt, \quad \text{with} \quad \Delta t = t_k - t_{k-1}, \quad (6)$$

where $\Omega(\omega)$ is a skew-symmetric matrix of input angular rates. The formulation of the angular rate as a control input allows us to preserve the highly dynamical motion of the foot without developing any explicit models. The angular rate in the expression above is:

$$\omega_k = \tilde{\omega}_k - b_{\omega,k-1} + w_{\omega,k}, \quad (7)$$

where $w_{\omega,k} \sim \mathcal{N}(0, Q_{\omega,k})$ is the gyroscope noise and $\tilde{\omega}_k$ corresponds to the actual output of the gyroscope. The acceleration measurement can be also treated as a control input:

$$a_k = \tilde{a}_k - b_{a,k-1} + w_{a,k}, \quad (8)$$

where $w_{a,k} \sim \mathcal{N}(0, Q_{a,k})$. The process models for the gyroscope and accelerometer biases are assumed to be:

$$b_{\omega,k} = b_{\omega,k-1} + w_{b_\omega,k}, \quad (9)$$
$$b_{a,k} = b_{a,k-1} + w_{b_a,k}, \quad (10)$$

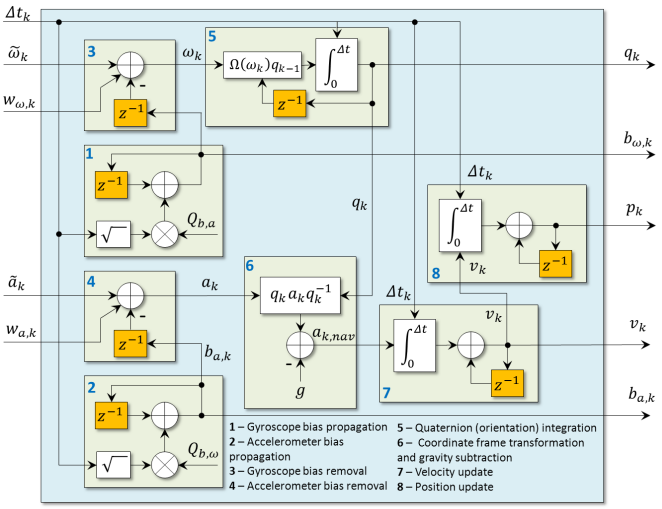

Figure 1. A sketch of the process model for prediction step in the UKF/EKF. Some unit delay blocks are omitted for simplicity.

with $w_{b_\omega,k} \sim \mathcal{N}(0, Q_{b_\omega,k})$ and $w_{b_{a,k}} \sim \mathcal{N}(0, Q_{b_a,k})$. The measured acceleration can be transformed to the navigation frame using:

$$a_{k,nav} = q_k a_k q_k^{-1} - g, \tag{11}$$

with $g \approx \begin{bmatrix} 0 & 0 & 9.81 \end{bmatrix}^T$ m/s^2. Then the velocity and the position are obtained by trapezoidal integration. The process as depicted in Fig. 1 does not consider the system initialization. In practice an extra noise can be added to the position estimate in order to take into account the unmodeled errors from the inertial navigation as well as failures in the stance phase detector.

We distinguish two different measurement model groups: one is called 'Zero Velocity Updates' and contains all updates which utilize the inertial sensors and the fact, that the human foot undergoes a still phase on a regular basis. The second group uses additional sensors such as magnetometers, barometers, an RFID reader and a GPS receiver. Under normal conditions, human walking follows a pattern similar to the one depicted in Fig. 2 (top). During the stance phase we assume that the foot is not moving and, therefore, the velocity of the foot has to be approximately zero. Similarly, the angular rate should be also close to zero for the no-motion conditions and the measured acceleration vector should contain only the terms due to gravity and the sensor biases. Under 'no motion' condition the following measurement models are adopted:

Zero Velocity Update (ZUPT): this is a pseudo measurement where we assume the velocity v_k to be zero when the associated conditions are fulfilled:

$$\begin{bmatrix} 0 & 0 & 0 \end{bmatrix}^T = v_k + \epsilon_{ZUPT,k}, \tag{12}$$

where the measurement noise $\epsilon_{ZUPT,k} \sim \mathcal{N}(0, R_{ZUPT})$ stands mainly for erroneous triggering within the detection mechanism.

Zero Angular Rate Update (ZARU): under 'no motion' condition the measured angular rate is due to sensor bias only:

$$\tilde{\omega}_k = b_{\omega,k} + \epsilon_{ZARU,k}, \tag{13}$$

with $\epsilon_{ZARU,k} \sim \mathcal{N}(0, R_{ZARU})$.

Gravity (G): we employ the acceleration measurement to compensate the pitch and roll under the conditions that no significant linear acceleration is present and the observations $\tilde{a}_k$ are solely due to measured gravity vector g and accelerometer bias:

$$\tilde{a}_k = q_k^{-1} g q_k + b_{a,k-1} + \epsilon_{G,k}, \tag{14}$$

where $\epsilon_{G,k} \sim \mathcal{N}(0, R_G)$.

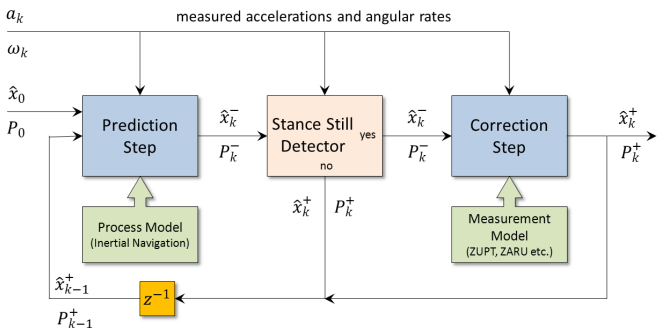

Figure 3. Block diagram of the filter for position estimation using ZUPT.

Different strategies have been proposed in the literature [13], [14], [19] for stance still detection (SSD). Although the pure inertial detection mechanisms are not completely reliable [15], we have found experimentally that a combination of three different detectors provides the best performance. Fig. 2 demonstrates the accelerometer and the gyroscope signals during a single step and three different detection conditions. The detection of the stance phase is implemented according to [13], where after one of the gyroscope or accelerometer signals have entered the predefined limits (the magnitude of the gyroscope signal below 0.1 rad/s, and the acceleration in the range from 9.6 to 10.0 m/s^2), a delay of 30 ms is imposed before the ZUPT or ZARU conditions are enabled. The values must stay within the ranges for the associated condition to be valid. If the delay requirement is satisfied, new thresholds are computed at each iteration using the current threshold and the actual sensor output. The detector is disabled when the signal values start to grow too fast as the foot is expected to enter the swing phase. Within our implementation the ZUPT and ZARU models are enabled and disabled separately, and when both conditions are simultaneously satisfied, the G measurement model is added. Fig. 3 shows a block diagram for the generic filtering approach. The process model is performed continuously using the INS-based model, while the detector checks if one of the still stance condition is satisfied. If so, the predicted state estimate $\hat{x}_k^-$ and corresponding covariance P_k^- are corrected using one of the measurements discussed above. However, if the detector fails to confirm the still condition, no correction is performed and the predicted values are considered as an input for the next filter cycle. Measurements from

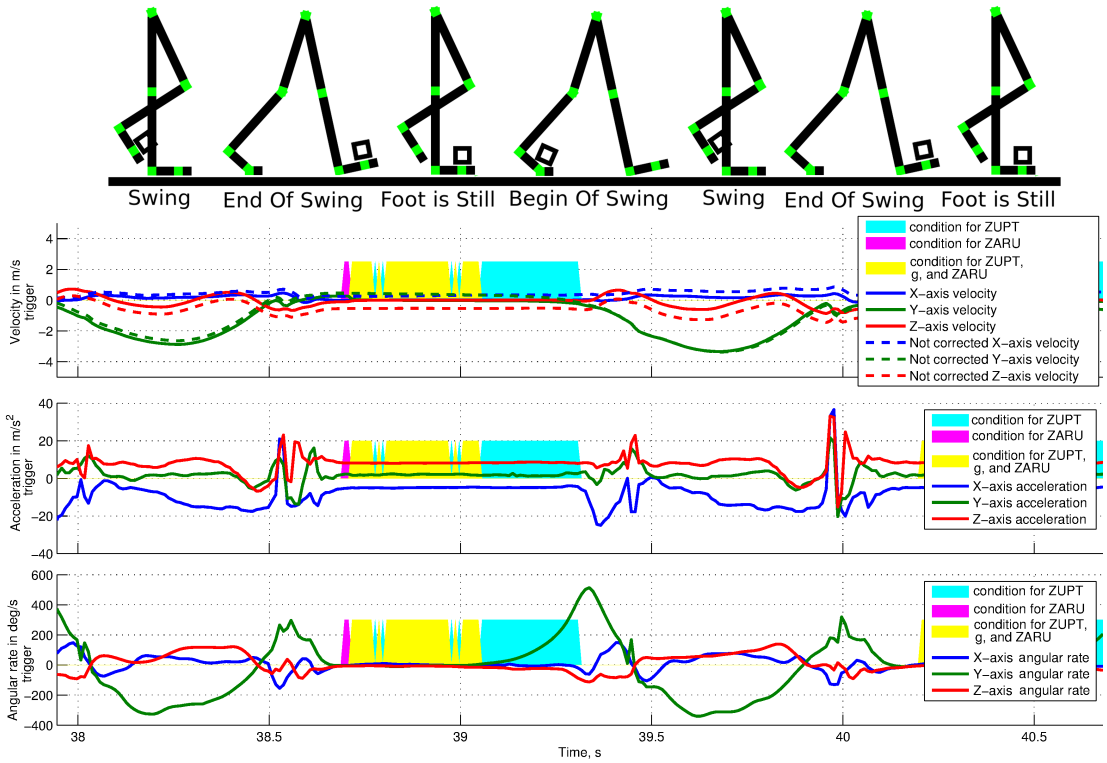

Figure 2. A sketch of the stance phases for human bipedal motion (top) and an example of stance still detection. The velocity plot also shows the drift of the estimated velocity if not corrected by the ZUPT mechanism.

additional sensors can be easily incorporated to the filter as explained below:

Magnetic Field Measurement: the magnetic field measurement model resembles those of the acceleration:

$$\tilde{m}_k = q_k^{-1} m q_k + \epsilon_{M,k}, \tag{15}$$

where m is the Earth's magnetic field at the given location and $\epsilon_{M,k} \sim \mathcal{N}(0, R_M)$. The magnetic field measurements can be performed continuously and are not conditioned on the foot motion phase.

Barometric Pressure Measurements: the following model for height measurement is adopted:

$$\tilde{p}_{z,k} = \frac{T_0}{L}\left(\left(\frac{S_k}{S_0}\right)^{-\frac{LR}{G}} - 1\right) + \epsilon_{h,k}, \tag{16}$$

where S_k is the barometric pressure. The model represents a simplified expression for altitude in terms of atmospheric pressure with the lapse rate $L = -6.5 \times 10^{-3}$ K/m and T_0 and S_0 for the temperature and base pressure at zero altitude, R - the gas constant for air and G for the gravity acceleration value [26]. For our scenarios with small vertical displacement we assume a linear additive noise model $\epsilon_{h,k} \sim \mathcal{N}(0, R_h)$ for the vertical position. A higher noise can be assumed for the height measurements due to environmental impact such as people moving around or opening/closing doors.

RFID: for the scenario with passive RFID tags we adopt a simple position measurement model:

$$\tilde{p}_k = p_k + \epsilon_{RF,k}. \tag{17}$$

with $\epsilon_{RF,k} \sim \mathcal{N}(0, R_{RF})$. Here the additive noise component represents the our ability to detect the tag when passing close to it and is experimentally chosen close to the RFID detection distance.

GPS: a similar position measurement model is assumed for segments with GPS available:

$$\tilde{p}_k = p_k + \epsilon_{GPS,k}. \tag{18}$$

with the position measurement uncertainty $\epsilon_{GPS,k} \sim \mathcal{N}(0, R_{GPS})$. Clearly, the GPS position noise can hardly satisfy the additive Gaussian white noise assumption of the KF and more elaborated models are often assumed for higher performance systems. For our scenario we impose a validation threshold on the GDOP value for the measurement to be accepted within the correction step. Unfortunately, the multipath and reflection errors are still not properly handled and can strongly affect the performance of the overall system when approaching the buildings.

IV. Hardware and System Concept

The purpose of the presented work is to demonstrate the feasibility of the approach using extremely low-cost off-the-shelf hardware with a general system concept to be found in Fig. 4. The system consists of a sensor unit placed on the foot with the sensor data to be continuously transmitted

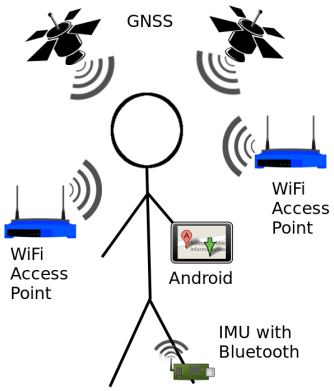

Figure 4. A general system concept.

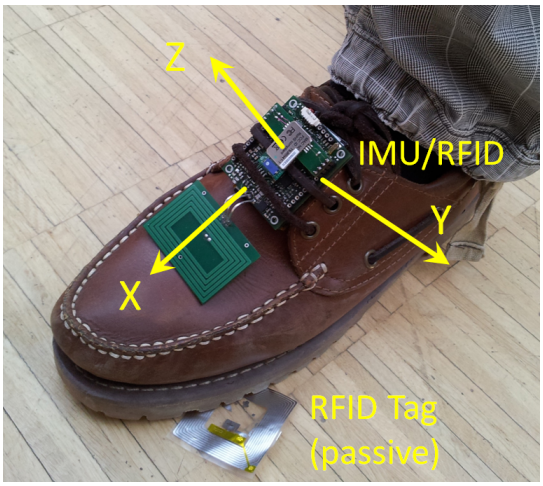

Figure 5. Custom IMU mounted on a foot with RFID reader antenna and passive tag beneath the foot.

to a Tablet PC via a Bluetooth interface. As an affordable computing platform we have chosen the Tablet PC running Android OS. The platform is also expected to have access to the map and environment information as well as GNSS and WiFi for absolute position referencing when applicable. The pure inertial sensing does not provide an initial position. This information has to be known in advance via other sensing mechanisms (GPS, WiFi) or explicitly set by the user via GUI. Note that the presented framework is rather general and will clearly perform better with higher quality and better calibrated sensors.

The foot-mounted hardware follows a modular approach where the core of the developed system consists of two main boards: the sensor unit and a power unit with the battery attached (see Fig. 5). The sensor unit contains the TI MSP430 MCU, responsible for sensor readout, data preprocessing and communication, a 3-axis accelerometer, a 3-axis gyroscope, a 3-axis magnetometer and a barometric pressure sensor. The inertial sensors are sampled at 100Hz, the magnetometer and the barometer are sampled at 75Hz and 2Hz respectively.

The sensor unit can also contain an RFID reader (13.56MHz chip carrier frequency, polling rate $\approx$ 50ms), while several

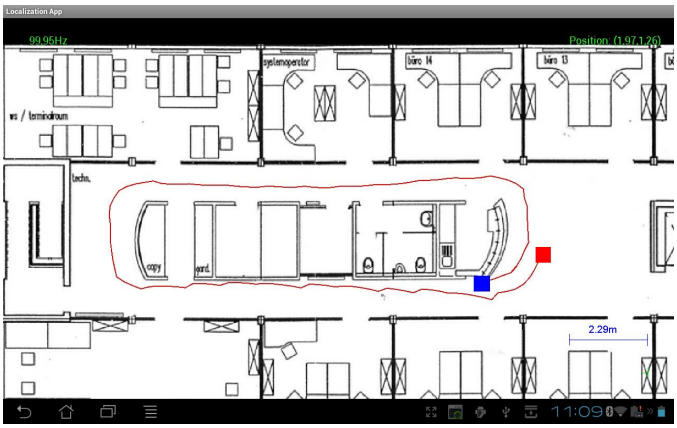

Figure 6. The indoor localization is visualized using an indoor map onto which the current position (marked by a blue square) and a part of the trajectory is plotted. Start position is marked as a red square.

passive RFID tags are distributed over the floor at known positions. When the user passes by a tag, its unique ID is retrieved and mapped to a particular location in the environment, correcting the accumulated position drift. The main advantage of the passive RFID tags is that they are extremely cheap and quick to install. For GPS measurements we used the built-in GPS module (reported to be a Broadcom BCM4751) in the Samsung Galaxy Tab (GT-P1010) running Android 2.2.1. A basic calibration of the magnetic field sensor is performed similarly to [12] in order to remove the influence of the setup. Similar calibration was adopted for accelerometer, while the default datasheet calibration was used for the gyroscope with a linear fit for the bias temperature dependence.

The filter algorithms as well as the graphical user interface were implemented in Java using the Android SDK [27]. After the startup the application attempts to connect via Bluetooth to the foot-mounted unit. On a successful connection three threads are created: one for reading Bluetooth data, one for the execution of the KF algorithm and a third one for updating the GUI and associated visualization. The communication between the threads is accomplished using handlers - which allows sending and process messages associated with a thread's MessageQueue [27]. For future platforms with multiple cores (e.g. Tegra^{TM} 3 from nVidia) the approach gives more processing power to the algorithm and ensures that no Bluetooth packets are lost along with a smooth and responsive GUI. Without the GPS, the correct initial position, orientation and scaling have to be provided by the user in a preference window. The length of the shown trajectory is also user adjustable. In the screenshot in Fig. 6 only the indoor localization scenario is depicted. Within our on-going work we are trying to combine the visualization of indoor and outdoor navigation in a consistent manner. The necessary transition between the lower resolution outdoor map and a more detailed indoor map can be dealt, for example, by using an appealing zoom and rotation animation.

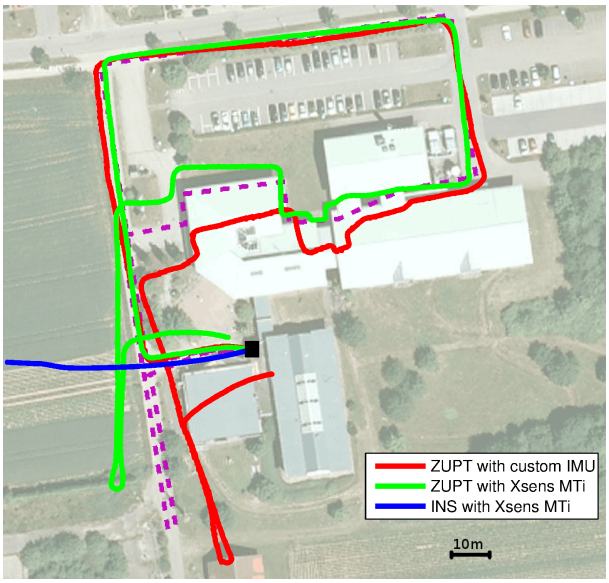

Figure 7. Pure inertial localization using the XSens MTi and HSG-IMIT custom inertial unit. Black square marks the start of walking while the pink dashed line corresponds to the true trajectory (duration appr. 5 minutes).

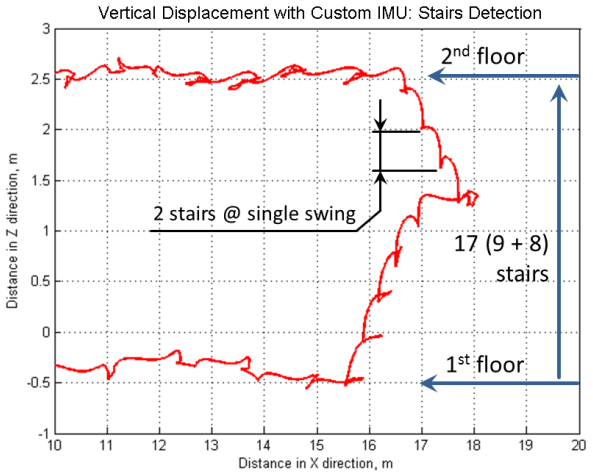

Figure 8. Vertical displacement scenario with stairs using a custom IMU.

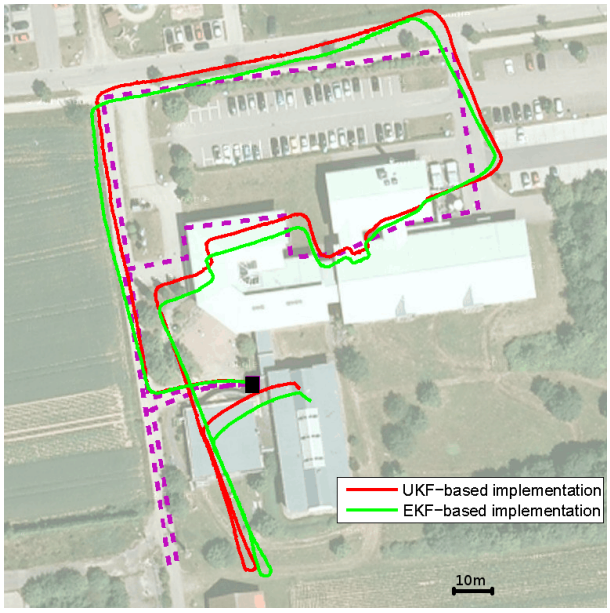

Figure 9. UKF and UKF based implementation of the inertial algorithm version. The pink dashed line corresponds to the true walking path.

V. Results and Discussion

The filter is initialized with the correct pitch and roll angles (quaternion equivalent) from the accelerometer and the gyroscope bias estimates obtained from the first several seconds while the user being still. The control noise for the accelerometer was set to $\sigma_a = 0.02\text{m/s}^2$ and for the gyroscope $\sigma_\omega = 3$ mrad/s. The G measurement model noise was set to $\sigma_G = 0.05$ m/s^2 due to additional uncertainty within the Stance Still Detector (SSD). The process noise for gyroscope bias was set to $\sigma_{b_\omega} = 3 \cdot 10^{-6}$ rad/s for $F_s = 100$Hz and accelerometer bias drift was modelled with $\sigma_{b_a} = 10^{-5}$ m/s^2. The measurement models were implemented assuming $\sigma_{ZUPT} = 2 \cdot 10^{-2}$ m/s, $\sigma_{ZARU} = 0.02$ rad/s. Both ZUPT and ZARU are pseudo measurements with the noises essentially representing the quality of the associated ZUPT and ZARU detectors.

IMU type Fig. 7 presents the results of with inertial-only approach for both XSens MTi (calibrated sensor data only) and our custom IMU. Although the MTi unit (price appr. 1500$) outperforms our custom IMU, the difference is not dramatic and even a low-cost system is able to provide a meaningful trajectory over a reasonably long period of time, while the direct INS mechanization fails to deliver a reliable position due to fast accumulating errors. The mismatch in the vertical position was between 1 and 2 meters for both systems, although the custom IMU had demonstrated more rugged vertical position estimation and several vertical jumps which could be also attributed to failures in SSD mechanism. The vertical accuracy of our IMU is enough to distinguish separate stairs (actually a couple of stairs as long as the unit is mounted on a single shoe and a single swing usually covers 2 stairs) as shown in Fig. 8.

EKF - UKF Fig. 9 compares 2 otherwise identical inertial-only algorithms based on EKF and UKF. Although the estimated trajectories are slightly different, both filters are able to provide a fairly good performance. The slight difference between the filters can be attributed to the fact that the estimated sensor biases are used as the inputs for SSD mechanism. Therefore, even slight differences in estimated biases are amplified via their influence on the SSD mechanism and associated trigger for correction step. For well-calibrated sensors with the SSD used without sensor biases, the differences in accuracy between UKF and EKF are believed to be considerably smaller as have to be caused solely by the statistical properties of the corresponding filters. The EKF-based scheme had shown up to 8x improvement in speed compared to our original UKF implementation on the same data sets when implemented in Java.

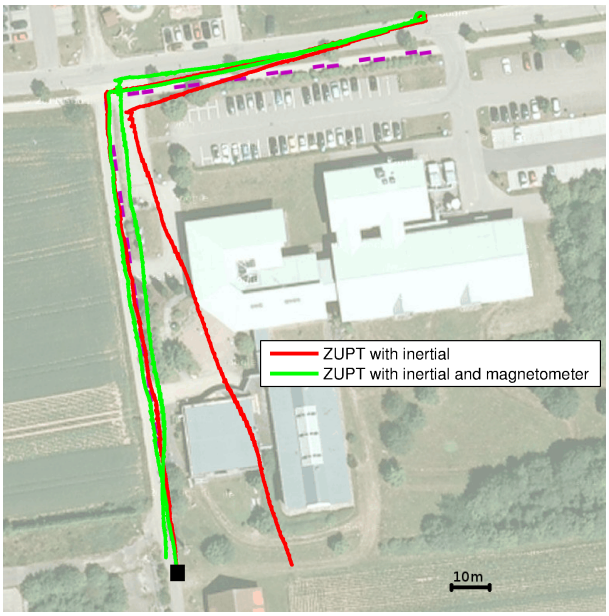

Figure 10. Comparison of the filter performance with and without magnetic field information. The pink dashed line corresponds to the true walking path.

Accelerometer bias The presence of the accelerometer bias in the system state slightly improves the position estimation when compared to a filter without the sensor offset estimation. However, this depends on the quality of the sensor and comes at a price of three extra states within the filter. Although the true sensor characteristics are often employed for noise covariance estimation, the situation is more delicate for the ZUPT/ZARU/G pseudo measurements, where the entire SSD mechanism can be considered as the sensor per se. Some extra tuning efforts required for these models can be also explained by the violation of the Gaussian additive noise assumption caused by heuristics in SSD mechanism. The issue is consistent with the results of other authors (e.g. see discussion in [21]).

Magnetometer Although the absolute heading information can be obtained by measuring the Earth's magnetic field, the measurements are usually unreliable for indoor environments due to correlation in errors caused by the furniture and infrastructure. These correlated errors are relatively large compared to the sensor intrinsic noise, usually are non-Gaussian and therefore a better compass with lower noise values will not result in improvement in the position accuracy. The issue is usually solved by assuming a larger measurement noise in order to allocate the possible disturbances and/or employing a heuristic detector conditioned on the measured field amplitude [18]. For outdoor scenarios with minor magnetic disturbances the situation is often better as one can see in Fig. 10.

G measurement From the results presented above it is not completely clear whether such a fairly complex ZUPT+ZARU+G SSD mechanism is necessary or a simplified approach can be used. Clearly, the ZUPT measurement model is crucial in order to limit the fast growing position error due to double integration of the accelerometer offset. Our experimental findings have confirmed that addition of the G measurement model strongly improves the performance as both pitch and roll angles become observable. The influence of the ZARU model was rather minor which could be attributed to the stability of the gyroscope bias during the short walk and good indirect observability of the bias from the G model.

Barometer A barometric pressure sensor can be used to eliminate the vertical position drift of a pure inertial system and, with some modifications, to determine a correct floor in a multi-storey building [4]. The pressure measurements are assumed to be valid only during the ZUPT+ZARU+G condition in order to minimize the disturbances induced by the air circulation while the foot is moving. The localization results for a multi-floor setup with an elevator/stairs segment are presented in Fig 11. Note that an elevator scenario was already addressed in [26] using both accelerometer and barometer, although no explicit localizaiton results had been provided. A pure inertial version fails to detect the elevator part, while the version with the barometer (σ_h = 0.2m) corrects the height estimation. A higher barometer noise is probably caused by the air circulation during the motion, opening/closing of the elevator doors, ventilation system etc. A faster height correction can be achieved with smaller σ_h values, while a higher uncertainty assigned to the barometer measurements increases a delay in height correction similar as shown for part A in Fig. 12, where the filter was too late to correct the vertical offset before the person left the elevator and returned to the starting point. Note that accuracy of our low-cost barometer was not sufficient to resolve the height of single stairs, although this was shown to be possible with inertial sensing as confirmed by Fig. 8. A better performance of barometer reported in [11] can be also attributed to the fact that MTi-G unit has a housing and influence of air circulation during the motion is reduced.

RFID By augmenting the system with an RFID reader one can address the issues of unbounded X-Y position errors (Fig. 13 and 14). The position of the detected passive RFID tags is uniquely defined via its ID and a direct position correction (with σ_{RF} = 0.1m) can be applied if the user steps on or close to the RFID tag. The performance of such a scheme strongly depends on the number of RFID tags encountered during the walking and one should intend to put the tags on commonly traversed locations. Note that not all the tags shown in Fig. 13 and 14 were detected and even few tags encountered during the path are able to significantly improve the quality of the estimated trajectory. A combination of an IMU and RFID is a perfect example of complementary sensing modalities where short term tracking between RFID detection events is supported by accurate absolute position information from the RFID tags.

GPS For a mixed indoor/outdoor scenario one of the simplest solutions is to augment the inertial system with the GPS position measurements. The performance of such a filter is shown in Fig. 15 and compared to the one of a pure inertial filter. The received GDOP (i.e. the satellite-receiver geometry)

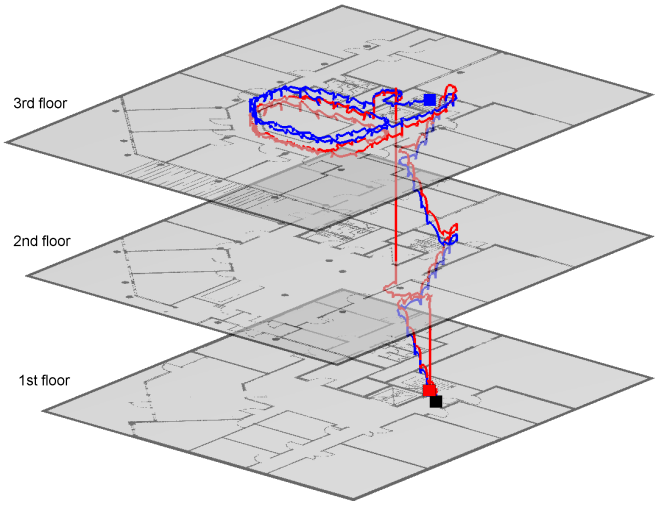

Figure 11. Multi-storey localization scenario with pure inertial ZUPT with (red line) and without (blue line) barometric pressure sensor. Perspective view for estimated path (vertical scale artificially increased to improve the separation between floors). Total walking duration appr. 3 minutes. Black square: start of the path; blue and red squares: end points for the associated filters.

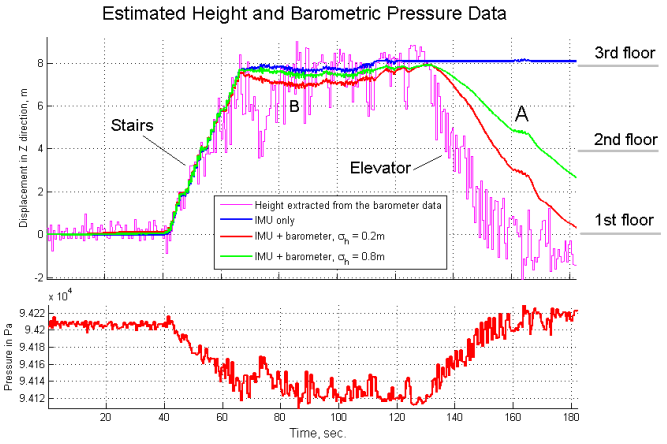

Figure 12. Height estimation results for multi-floor scenario and barometric pressure data.

value is used as indicator of the measurement quality with a threshold value of 5 meters set for the measurement to be considered eligible. While the outdoor trajectory segment is corrected by the GPS measurements, the indoor segment also benefits from previous GPS measurement due to decreased heading drift and smaller position mismatch when entering the building. Note that the GPS measurements were assumed slightly worse as they truly are to avoid jumpy corrections for outdoor segments.

VI. Concluding Remarks and Outlook

Within the work we have experimentally investigated a performance of a low-cost foot-mounted inertial unit for mixed indoor/outdoor scenarios and continuous localization over a longer period of time. A number of additional sensors such as magnetometers, barometric pressure sensor, RFID tag reader

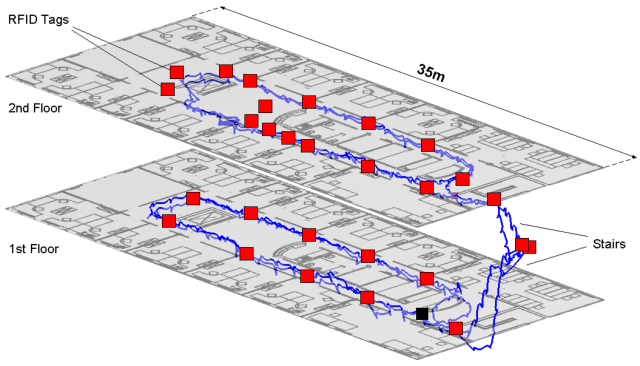

Figure 13. System performance with RFID reader for multi-floor scenario. Red squares mark the position of RFIDs while the black square denotes the start of the walking. The vertical scale is artificially increased for improved visual separation between the floors.

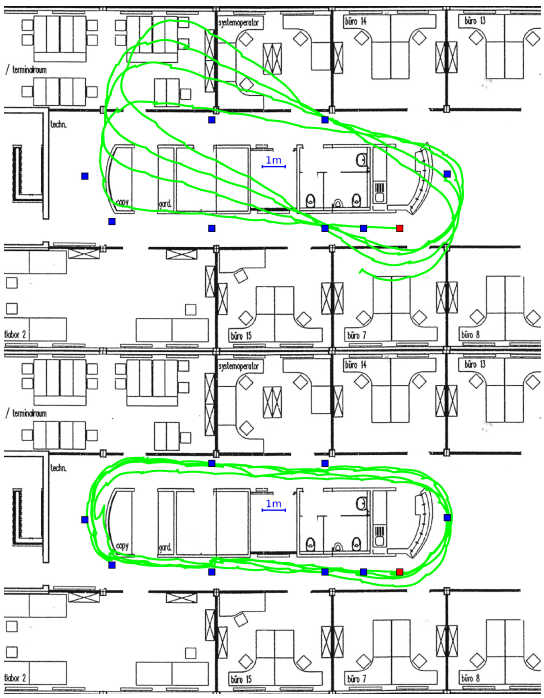

Figure 14. Pure inertial localization (top) and approach with RFID measurements (bottom) for a single floor scenario. Blue squares mark the positions of RFID tags while the red square denotes the start of the walking path.

and GPS have been attached in order to address the drawbacks of a pure inertial approach and to increase the robustness of the complete system.

As the system is intended to operate on Android OS based smartphones and Tablet PCs, one expects further improvement in performance if Wi-Fi RSSI measurements are added to the system and available map information is integrated to the filter. Here the map constraints can be incorporated either via constrained versions of KF or by adopting a hybrid estimation strategy, where a modification of an UKF/EKF or is adopted as a proposal density function within the Particle Filter (PF), where marginalized PF can be an alternative solution. The approach would allow to represent multiple position hypothesis

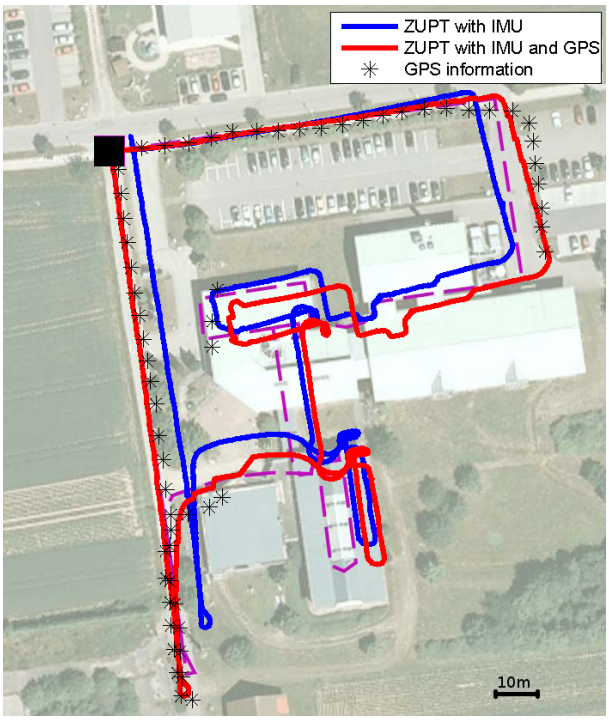

Figure 15. Pure inertial localization with and without GPS measurements. The pink dashed line corresponds to the true walking path.

which can arise due to symmetry of the maps and still keep our filter computationally tractable. Some further work is also planned on better models for the GPS noise and significant improvement in computational performance is expected with rewriting the UKF/EKF with C/C++ using Android Native Development Kit (NDK).

References

[1] H.-S. Ahn and W. Yu, "Indoor mobile robot and pedestrian localization techniques," in *Control, Automation and Systems, 2007. ICCAS '07. International Conference on*, oct. 2007, pp. 2350 –2354.

[2] S. Thrun, W. Burgard, and D. Fox, *Probabilistic Robotics (Intelligent Robotics and Autonomous Agents)*. The MIT Press, September 2005.

[3] G. Glanzer, T. Bernoulli, T. Wiessflecker, and U. Walder, "Semi-autonomous indoor positioning using MEMS-based inertial measurement units and building information," in *Positioning, Navigation and Communication, 2009. WPNC 2009. 6th Workshop on*, march 2009, pp. 135 –139.

[4] G. Retscher, "Location determination in indoor environments for pedestrian navigation," in *Position, Location, And Navigation Symposium, 2006 IEEE/ION*, 25-27, 2006, pp. 547 – 555.

[5] R. Mautz, "The challenges of indoor environments and specification on some alternative positioning systems," in *Positioning, Navigation and Communication, 2009. WPNC 2009. 6th Workshop on*, march 2009, pp. 29 –36.

[6] S.-W. Lee and K. Mase, "Activity and location recognition using wearable sensors," *Pervasive Computing, IEEE*, vol. 1, no. 3, pp. 24 – 32, 2002.

[7] S. House, S. Connell, I. Milligan, D. Austin, T. Hayes, and P. Chiang, "Indoor localization using pedestrian dead reckoning updated with RFID-based fiducials," in *Engineering in Medicine and Biology Society,EMBC, 2011 Annual International Conference of the IEEE*, 30 2011-sept. 3 2011, pp. 7598 –7601.

[8] C. Laderriere, M. Heddebaut, J. Prost, A. Rivenq, F. Elbahhar, and J. Rouvaen, "Wide-band indoor localization effectiveness in presence of moving people," in *Positioning, Navigation and Communication, 2008. WPNC 2008. 5th Workshop on*, march 2008, pp. 103 –111.

[9] D. Harmer, A. Yarovoy, N. Schmidt, K. Witrisal, M. Russell, E. Frazer, T. Bauge, S. Ingram, A. Nezirovic, A. Lo, L. Xia, B. Kull, and V. Dizdarevic, "An ultra-wide band indoor personnel tracking system for emergency situations (Europcom)," in *Radar Conference, 2008. EuRAD 2008. European*, oct. 2008, pp. 404 –407.

[10] G. Retscher and Q. Fu, "Continuous indoor navigation with RFID and INS," in *Position Location and Navigation Symposium (PLANS), 2010 IEEE/ION*, may 2010, pp. 102 –112.

[11] R. Feliz, E. Zalama, and J. Gmez, "Pedestrian tracking using inertial sensors," *Journal of Physical Agents*, vol. 3, no. 1, pp. 35–43, 2009. [Online]. Available: http://www.jopha.net/index.php/jopha/article/view/35

[12] L. Klingbeil, M. Romanovas, P. Schneider, M. Traechtler, and Y. Manoli, "A modular and mobile system for indoor localization," in *Indoor Positioning and Indoor Navigation (IPIN), 2010 International Conference on*, sept. 2010, pp. 1 –10.

[13] E. Foxlin, "Pedestrian tracking with shoe-mounted inertial sensors," *Computer Graphics and Applications, IEEE*, vol. 25, no. 6, pp. 38–46, Nov.-Dec. 2005.

[14] K. Abdulrahim, C. Hide, T. Moore, and C. Hill, "Aiding MEMS IMU with building heading for indoor pedestrian navigation," in *Ubiquitous Positioning Indoor Navigation and Location Based Service (UPINLBS), 2010*, oct. 2010, pp. 1 –6.

[15] O. Bebek, M. Suster, S. Rajgopal, M. Fu, X. Huang, M. Cavusoglu, D. Young, M. Mehregany, A. van den Bogert, and C. Mastrangelo, "Personal navigation via shoe mounted inertial measurement units," in *Intelligent Robots and Systems (IROS), 2010 IEEE/RSJ International Conference on*, oct. 2010, pp. 1052 –1058.

[16] J. Bird and D. Arden, "Indoor navigation with foot-mounted strapdown inertial navigation and magnetic sensors [emerging opportunities for localization and tracking]," *Wireless Communications, IEEE*, vol. 18, no. 2, pp. 28 –35, april 2011.

[17] B. Krach and P. Robertson, "Integration of foot-mounted inertial sensors into a Bayesian location estimation framework," in *Positioning, Navigation and Communication, 2008. WPNC 2008. 5th Workshop on*, march 2008, pp. 55 –61.

[18] W. T. Faulkner, R. Alwood, D. W. Taylor, and J. Bohlin, "GPS-denied pedestrian tracking in indoor environments using an IMU and magnetic compass," in *Proceedings of the 2010 International Technical Meeting of The Institute of Navigation*. San Diego, CA: ION, January 2010, pp. 198–204.

[19] A. Jimenez, F. Seco, C. Prieto, and J. Guevara, "A comparison of pedestrian dead-reckoning algorithms using a low-cost MEMS IMU," in *Intelligent Signal Processing, 2009. WISP 2009. IEEE International Symposium on*, aug. 2009, pp. 37 –42.

[20] A. Jimenez, F. Seco, J. Prieto, and J. Guevara, "Indoor pedestrian navigation using an INS/EKF framework for yaw drift reduction and a foot-mounted IMU," in *Positioning Navigation and Communication (WPNC), 2010 7th Workshop on*, march 2010, pp. 135 –143.

[21] D. Chdid, R. Oueis, H. Khoury, D. Asmar, and I. Elhajj, "Inertial-vision sensor fusion for pedestrian localization," in *Robotics and Biomimetics (ROBIO), 2011 IEEE International Conference on*, dec. 2011, pp. 1695 –1701.

[22] D. Fox, J. Hightower, L. Liao, D. Schulz, and G. Borriello, "Bayesian filtering for location estimation," *Pervasive Computing, IEEE*, vol. 2, no. 3, pp. 24 – 33, july-sept. 2003.

[23] R. van der Merwe and E. Wan, "Sigma-point Kalman filters for integrated navigation," in *Proceedings of the 60th Annual Meeting of The Institute of Navigation (ION)*, Dayton, Ohio, June 2004, pp. 1 – 14.

[24] M. Romanovas, L. Klingbeil, M. Traechtler, and Y. Manoli, "Efficient orientation estimation algorithm for low cost inertial and magnetic sensor systems," in *2009 IEEE Workshop on Statistical Signal Processing*. Cardiff, Wales, UK: IEEE, 2009.

[25] S. Julier, "The spherical simplex unscented transformation," in *American Control Conference, 2003. Proceedings of the 2003*, vol. 3, june 2003, pp. 2430 – 2434 vol.3.

[26] Y. Chen, R. Chen, L. Pei, T. Kroger, H. Kuusniemi, J. Liu, and W. Chen, "Knowledge-based error detection and correction method of a multi-sensor multi-network positioning platform for pedestrian indoor navigation," in *Position Location and Navigation Symposium (PLANS), 2010 IEEE/ION*, may 2010, pp. 873 –879.

[27] Google Inc. and the Open Handset Alliance. (2011) Android sdk - api libraries and developer tools necessary to build, test, and debug apps for android. http://developer.android.com/sdk/index.html. [Online]. Available: http://developer.android.com/sdk/index.html